International Journal of Biological Macromolecules 117 (2018) 565–573

Contents lists available at ScienceDirect

International Journal of Biological Macromolecules

journal homepage: http://www.elsevier.com/locate/ijbiomac

Cloning of cDNA sequences encoding cowpea (*Vigna unguiculata*) vicilins: Computational simulations suggest a binding mode of cowpea vicilins to chitin oligomers

Antônio J. Rocha [a], Bruno L. Sousa [b], Matheus S. Girão [a], Ito L. Barroso-Neto [c], José E. Monteiro-Júnior [d], José T.A. Oliveira [a], Celso S. Nagano [e], Rômulo F. Carneiro [e], Ana C.O. Monteiro-Moreira [f], Bruno A.M. Rocha [a], Valder N. Freire [g], Thalles B. Grangeiro [d,*]

[a] Departamento de Bioquímica e Biologia Molecular, Universidade Federal do Ceará (UFC), Fortaleza, CE 60440-900, Brazil
[b] Faculdade de Filosofia Dom Aureliano Matos, Universidade Estadual do Ceará, Av. Dom Aureliano Matos, 2060, Limoeiro do Norte, CE 62930-000, Brazil
[c] Departamento de Química Analítica e Físico-química, UFC, Fortaleza, CE 60455-760, Brazil
[d] Departamento de Biologia, UFC, Fortaleza, CE 60440-900, Brazil
[e] Departamento de Engenharia de Pesca, UFC, Fortaleza, CE 60440-900, Brazil
[f] Núcleo de Biologia Experimental, Universidade de Fortaleza, Fortaleza, CE 60811-905, Brazil
[g] Departamento de Física, UFC, Fortaleza, CE 60440-760, Brazil

ARTICLE INFO

Article history:
Received 14 March 2018
Received in revised form 25 May 2018
Accepted 26 May 2018
Available online 27 May 2018

Keywords:
Seed storage proteins
Chitin-binding proteins
Callosobruchus maculatus

ABSTRACT

Vicilins are 7S globulins which constitute the major seed storage proteins in leguminous species. Variant vicilins showing differential binding affinities for chitin have been implicated in the resistance and susceptibility of cowpea to the bruchid *Callosobruchus maculatus*. These proteins are members of the cupin superfamily, which includes a wide variety of enzymes and non-catalytic seed storage proteins. The cupin fold does not share similarity with any known chitin-biding domain. Therefore, it is poorly understood how these storage proteins bind to chitin. In this work, partial cDNA sequences encoding β-vignin, the major component of cowpea vicilins, were obtained from developing seeds. Three-dimensional molecular models of β-vignin showed the characteristic cupin fold and computational simulations revealed that each vicilin trimer contained 3 chitin-binding sites. Interaction models showed that chito-oligosaccharides bound to β-vignin were stabilized mainly by hydrogen bonds, a common structural feature of typical carbohydrate-binding proteins. Furthermore, many of the residues involved in the chitin-binding sites of β-vignin are conserved in other 7S globulins. These results support previous experimental evidences on the ability of vicilin-like proteins from cowpea and other leguminous species to bind *in vitro* to chitin as well as *in vivo* to chitinous structures of larval *C. maculatus* midgut.

1. Introduction

Cowpea [*Vigna unguiculata* (L.) Walp.] is an important food crop that is cultivated in arid and semi-arid regions of Africa, Asia and the Americas [1]. This leguminous species is adapted to high temperatures, drought and other abiotic stresses, and their dry seeds constitute a valuable source of proteins and calories for human consumption, especially for smallholder farmers [2]. One major constraint to cowpea production in developing countries is the attack by the bruchid beetle *Callosobruchus maculatus* (F.), commonly known as the cowpea weevil, which is a cosmopolitan pest of stored cowpeas. Fertilized females of *C. maculatus* lay their eggs on the surface of the seeds, usually a single egg per seed. Eggs hatch after 5–6 days of oviposition and the first-instar larvae burrow directly into the seed. Each developing larva feeds within a single seed, excavating a chamber as it grows. All larval stages and pupation occur within a single seed. At 25 °C and 70% relative humidity, adults emerge approximately 36 days after the eggs were laid [3]. Adults live on average 12–14 days, and during this time, they mate and the fertilized females lay eggs on undamaged seeds. Infestation of this bruchid species starts in the field and continues in storage, causing sometimes the complete destruction of seeds within a period of 3–4 months through secondary infestation [4]. Damaged seeds are unsuitable for human or animal consumption, have a decreased germination potential, lower nutritional qualities and a reduction in commercial value [5,6]. Due to financial and technical limitations, insect-resistant varieties would be the most effective method of controlling the cowpea weevil in northeastern Brazil and other underdeveloped regions of the world.

* Corresponding author at: Departamento de Biologia, Centro de Ciências, Universidade Federal do Ceará, Campus do Pici, Fortaleza, CE 60440-900, Brazil.
E-mail address: thalles@ufc.br (T.B. Grangeiro).

https://doi.org/10.1016/j.ijbiomac.2018.05.197
0141-8130/

In the 1970's, researchers at the International Institute of Tropical Agriculture (IITA) in Ibadan, Nigeria, initiated a systematic screening of over 8000 germplasm accessions of cowpea, aiming to develop bruchid resistant varieties. These efforts allowed the identification of three cowpea accessions, TVu 2027, TVu 11952 and TVu 11953, which showed moderately seed resistance to *C. maculatus* [7]. These accessions showed similar levels of resistance, in which the percentage of adult emergence was delayed, staggered and lower in comparison to the same parameters obtained for insects reared on susceptible seeds. Using these resistant genotypes, especially TVu 2027, several improved breeding lines combining resistance to *C. maculatus* with other desirable traits have been developed [8]. Gatehouse et al. were the first to hypothesize that resistance to cowpea weevil in TVu 2027 was due to elevated levels of trypsin inhibitors [9,10]. However, this claim was not supported by further experimental evidences, which have shown that the levels of proteinase inhibitors targeting different types of *C. maculatus* midgut proteases or even α-amylase inhibitors are not correlated with the resistance or susceptibility to bruchid infestation [11–14]. On the other hand, some authors have shown that cowpea vicilins purified from resistant lines derived from TVu 2027 are detrimental to *C. maculatus* larvae, and these vicilin variants are more refractory to digestion by the bruchid's midgut proteinases in comparison to vicilins from susceptible lines [15,16]. Furthermore, it has been shown that cowpea vicilins bind *in vitro* to chitin [17] and *in vivo* to chitinous structures of the midgut of *C. maculatus* larvae [18,19]. Binding of cowpea vicilins to larval midgut epithelial cell surface leads to the absorption of intact molecules and their transport into the haemolymph, fat body cells and Malpighian tubules [20]. Vicilin molecules are detected in these organs in all larval stages and pupae, and vicilin-derived peptides are also found in fat bodies of male and female adults, even 10 days after emergence [21]. Recent data have demonstrated that internalization of vicilin molecules in the enterocytes of *C. maculatus* larvae is accomplished predominantly through receptor-mediated, clathrin-independent endocytosis and vesicular trafficking in the cytoplasm [22,23]. A protein homologous to α-tocopherol transfer protein was identified as a putative membrane-bound vicilin receptor from larval *C. maculatus* enterocytes [23]. These findings have lead to the hypothesis that once internalized, variant vicilins disturb the normal physiology of *C. maculatus* enterocytes, adversely affecting the larval development. In this proposed mechanism, interaction of vicilins with protein receptors on the epithelial cells is a crucial step, that ultimately provoke the toxic effects of cowpea vicilins on developing larvae of *C. maculatus*. It is noteworthy to mention that cowpea vicilins did not show deleterious effects on larval development of *Zabrotes subfasciatus* [24], a bruchid species that usually attacks the seeds of common bean (*Phaseolus vulgaris*), but that is also able to successfully infest cowpea seeds [25].

Vicilins are 7S seed storage globulins that contain two copies of the cupin superfamily domain. The cupin domain is characterized by a double-stranded β-helix fold, which is found in diverse enzymes as well as in non-catalytic seed storage proteins [26]. However, there is no structural similarity between the cupin domain and known chitin-binding proteins, such as hevein and chitin-binding lectins, for example. These canonical chitin-binding proteins have typical carbohydrate-binding sites that recognize and bind one or more residues of *N*-acetyl-D-glucosamine (GlcNAc), the repeating unit of chitin. Therefore, the molecular mechanism involved in the interaction between cowpea vicilins and chitin oligomers remains poorly understood. In the present work, partial cDNA sequences encoding cowpea vicilins were obtained from genotypes EPACE-10 and IT81D-1053. Three-dimensional molecular models were generated, validated and subjected to molecular docking calculations and molecular dynamics simulations, aiming to reveal the putative chitin-binding sites in the modeled vicilin structures.

2. Materials and methods

2.1. Plant material

Cowpea seeds (genotypes IT81D-1053 and EPACE-10) were kindly provided by F. R. Freire-Filho (Embrapa Meio-Norte, Teresina-PI, Brazil) and E. M. Teofilo (Centro de Ciências Agrárias, UFC, Fortaleza-CE, Brazil), respectively.

2.2. Plasmid, bacterial strain and reagents

The plasmid pGEM-T Easy and cells of *Escherichia coli* strain TOP10F′ were purchased from Promega (Madison, WI, USA) and Invitrogen (Carlsbad, CA, USA), respectively. All other reagents were of analytical grade.

2.3. RNA purification, cDNA synthesis, amplification and cloning of PCR products

Total RNA was purified from developing seeds (harvested 12 days after pollination), using the method described by Chang et al. [27]. Conversion of total RNA to DNA was performed as previously described [28]. First-strand cDNA products were then amplified by polymerase chain reaction (PCR) using the following oligonucleotide primers: 5′-ATTG TACACCGGGAGCACCAAG-3′ (forward) and 5′-GTAGARASTGYCCAA AATWGAAGATAA-3′ (reverse). These primers were designed according to expressed sequence tags (ESTs) from cowpea, deposited in the NCBI's EST database (www.ncbi.nlm.nih.gov/dbEST/). The ESTs that encoded amino acid sequences matching the N- and C-terminal ends of characterized vicilins from related leguminous species were used to design the forward and reverse primers, respectively. Amplification reactions and cloning of PCR products into the pGEM-T Easy vector were performed as previously described [28].

2.4. DNA sequencing and sequence analysis

DNA sequencing was performed at the Macrogen Inc. (Seoul, South Korea) using the Sanger's dideoxy chain termination method. DNA sequencing and sequence assembly were done as described elsewhere [28]. Nucleotide sequences were translated to amino acid sequences using the ExPASy Translate tool (web.expasy.org/translate/). Manipulation, edition and alignment of sequences were performed using the program BioEdit v. 7.2.5 [29]. Searches for homologous sequences in public databases were performed using BLAST [30].

2.5. Purification of cowpea vicilins

Cowpea vicilins were extracted from seed flour according to the protocol first described by Samour et al. [31] and including the modifications described by Macedo et al. [16]. The preparations were further purified by size exclusion chromatography on Sephacryl S-200 and ion exchange chromatography on DEAE-Sepharose. Protein fractions were analyzed by SDS-polyacrylamide gel electrophoresis according to the method of Laemmli [32], using 15% slab gels. Staining and destaining of protein bands were performed as described by Lobo et al. [33]. N-terminal amino acid sequencing of protein bands resolved by SDS-PAGE was performed as described by Landim et al. [34].

2.6. Mass spectrometry analysis

Proteins were resolved by SDS-PAGE and electrophoretic bands were subjected to in-gel digestion with trypsin (Promega), according to the protocol previously described [35]. Identification of tryptic peptides by tandem mass spectrometry (LC-ESI-MS/MS) was performed using a Synapt G1 HDMS Q-ToF mass spectrometer (Waters Co., Milford, MA, USA) coupled to a Waters ultra-high-performance liquid

chromatography (UPLC) unit. Data processing, MS/MS ions search and peptide identification were done as described in detail by Freire et al. [36]. Tryptic peptides were also subjected to MALDI-TOF/TOF MS analysis (AutoFlex III mass spectrometer, Bruker Daltonics, USA). The spectrometer was operated in the reflector mode for MALDI-TOF MS peptide mass fingerprint (PMF), at *m/z* range of 700 to 4000, and in the "LIFT™" mode for MALDI-TOF/TOF MS/MS fragmentation experiments (at *m/z* range of precursor). Spectra were processed with Flex Analysis 3.4 software. PMF spectra were compared with *in silico* digestions of vicilin sequences using PEPTIDEMASS through the ExPASy server [37]. MS/MS spectra were interpreted manually. The ambiguities for isobaric amino acids were approached by amino acid sequences deduced from cDNA. Sequenced peptides were searched online against NCBI and UniProtKB databases.

2.7. Molecular modeling

Three-dimensional molecular models were generated using MODELLER [38] through the MPI Bioinformatics Toolkit [39] web service (toolkit.tuebingen.mpg.de). The crystal structure of the 7S globulin-1 (PDB ID: 2EA7) from adzuki bean (*V. angularis*) was used as template [40]. Models generated using MODELLER were refined using GalaxyRefine [41] through the program's web server. Refined models were validated concerning their stereo-chemical properties (Ramachandran plots, steric overlaps, Cβ deviation parameters, rotamers, and bond angle quality) using MolProbity [42] through the software's web server (molprobity.biochem.duke.edu/). Molecular images were prepared and rendered using the PyMOL Molecular Graphics System, version 1.7.4 (Schrodinger, LLC).

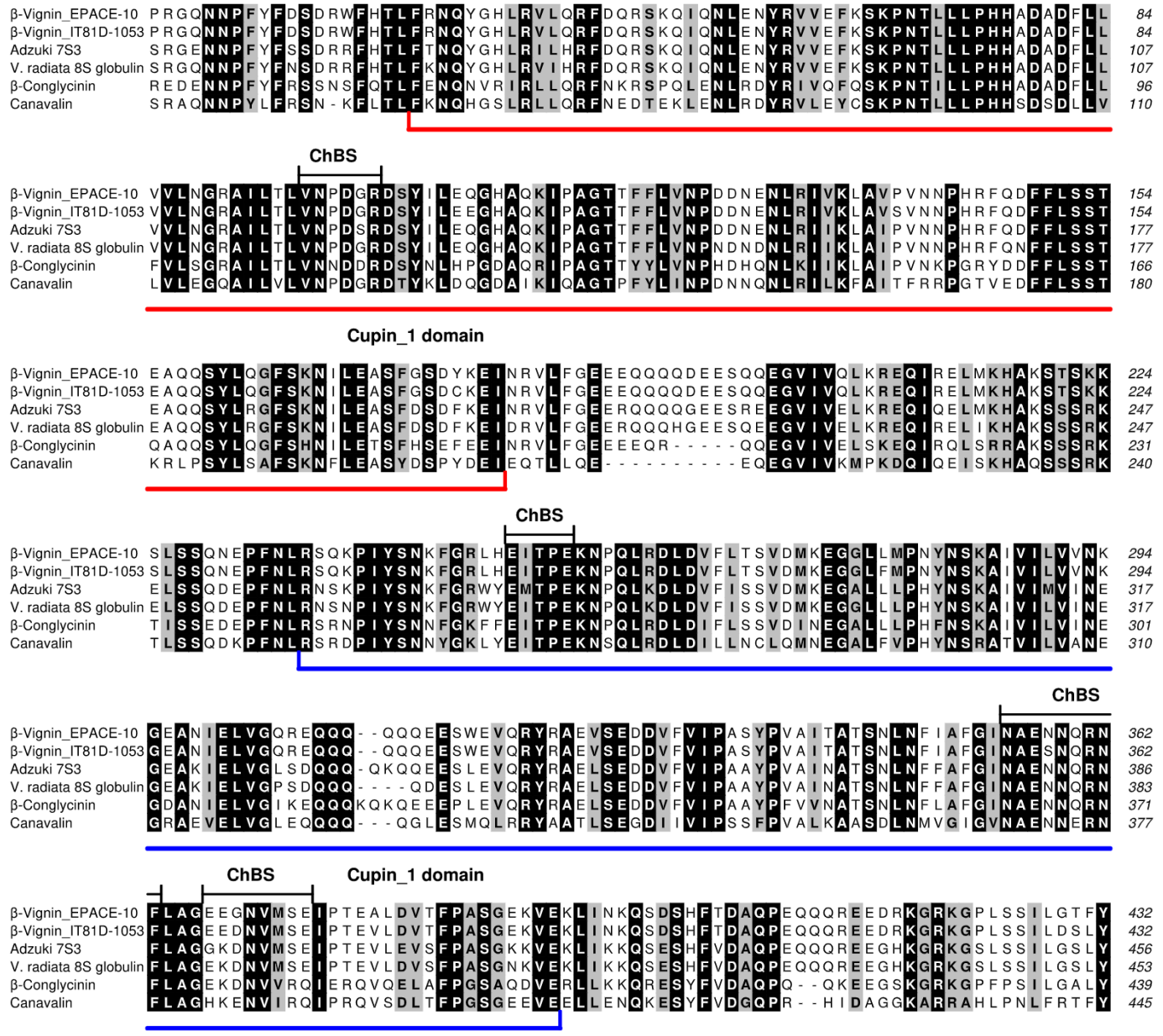

Fig. 1. Multiple sequence alignment of the amino acid sequences of β-vignin with the primary structures of representative vicilin-like 7S globulins. Amino acid sequences of β-vignin obtained from *V. unguiculata* genotypes EPACE-10 (sequence S2) and IT81D-1053 (sequence R2) were aligned with those of *V. angularis* (adzuki bean) 7S globulin-3 (Adzuki 7S3; UniProtKB accession number: A0A0S3SX36), *V. radiata* 8S globulin (UniProtKB accession number: Q198W3), β-conglycinin (from *Glycine max*; UniProtKB accession number: P25974) and canavalin (from *Canavalia ensiformis*; UniProtKB accession number: P50477). Segments in the primary structures of β-vignin that were shown to contribute to their chitin-binding site (ChBS), as evidenced by computational simulations, are indicated. The alignment was edited using the program ALINE [64].

2.8. Molecular docking calculations

A standard docking procedure was performed with AutoDock Vina v1.1.2 [43]. Initially, a blind docking strategy was performed using a search space defined by a 40 Å × 40 Å × 40 Å cube, which was applied to three different portions of each vicilin monomer, thus covering the whole protein surface. The ligands were $(GlcNAc)_4$ and $(GlcNAc)_5$, which were built using the program SWEET [44]. All of the torsional bonds of the ligands were free to rotate while the protein atoms were held rigid. Polar hydrogen atoms were added using the AutoDock Tools version 1.5.6, and Kollman united atom partial charges were assigned [45]. Afterwards, a refined search with the same ligands was performed using a search space defined by a 20 Å × 20 Å × 20 Å cube, based on the oligosaccharides length, centered on the top-ranked chitin binding site. Exhaustiveness was set to 15, and for all other parameters, default values were used. Selection of the best results was done as previously described [28].

2.9. Molecular dynamics (MD) simulations

MD simulations (30 ns) were performed using the program NAMD v2.10 (Nanoscale Molecular Dynamics) [46], with the force fields CHARMM27 [47] and CHARMM36 [48]. The software VMD (Visual Molecular Dynamics) was used for file preparation [49]. All MD simulations were performed essentially as described in detail by Maranhão et al. [28].

2.10. Binding energy calculations

Binding energy calculations were done using a dispersion-corrected density functional theory (DFT-D) method [50], using the procedure described in detail by Maranhão et al. [28].

3. Results and discussion

3.1. Cloning of partial cDNA fragments encoding β-vignin, the major vicilin from cowpea

PCR products with approximately 1200 bp that presumptively encoded vignin were amplified from total cDNA, which was obtained from developing seeds of cowpea genotypes EPACE-10 and IT81D-1053 (Fig. S1). Several clones were sequenced and 3 unique partial cDNA sequences from each genotype were identified. These sequences are herein referred to as S1, S2 and S3 from EPACE-10, which is

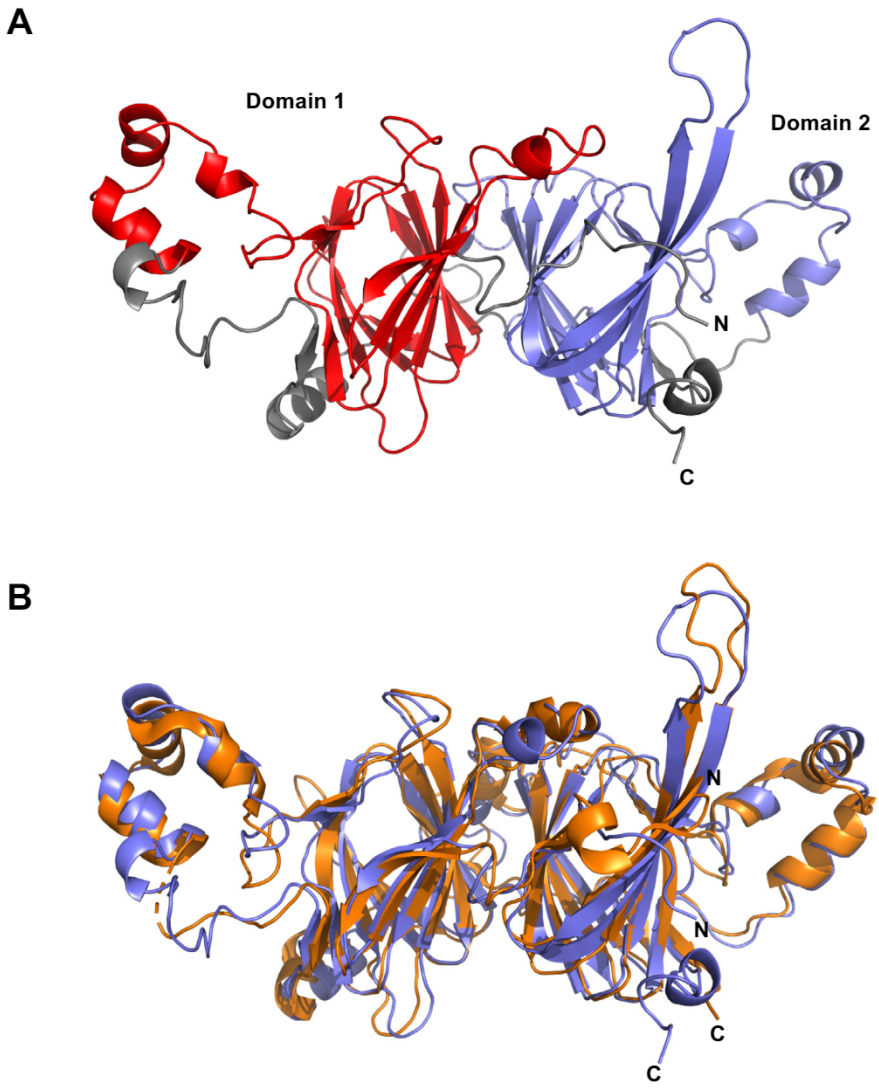

Fig. 2. Three-dimensional molecular model of β-vignin. N- and C-terminal cupin_1 domains are colored red and blue, respectively. (A) Ribbon diagram of the β-vignin monomer structure, as obtained by homology modeling from sequence R2. (B) Superposition of the β-vignin model (blue) over the x-ray crystallographic structure of the *V. angularis* 7S globulin-1 (orange), which was used as template (PDB ID: 2EA7). (For interpretation of the references to color in this figure legend, the reader is referred to the web version of this article.)

susceptible to *C. maculatus*, and R1, R2 and R3 from IT81D-1053, which is resistant to *C. maculatus*. All cDNA sequences were 1296 nucleotides long, except sequence S3, which had a length of 1287 nucleotides (Figs. S2–S7). Sequence identity ranged from 99.9% (1 different nucleotide), between S1 and R1, to 98.6% (17 distinct nucleotides), between R2 and R3 (Table S1). Sequence S3 encoded a polypeptide chain with 429 amino acid residues, whereas the other 5 sequences encoded proteins with 432 residues. The shorter sequence S3 was due to a deletion of 9 nucleotides (Fig. S8), encoding a stretch of 3 amino acid residues (^{193}QDE^{195} in the other 5 sequences) (Fig. S9). Vicilin-like 7S globulins are encoded by multigene families [51], and the mRNAs identified in the present work are likely the products of closely related cowpea genes. Pairwise comparisons revealed that the amino acid sequences of S1 and R1 were identical, whereas the other pairs of compared structures had differences, ranging from 3 to 11 residues (Table S2). Molecular masses calculated from these amino acid sequences varied from 49,347.02 (S3) to 49,827.45 Da (S1 and R1) (Table S3). BLASTp searches against the NCBI protein database revealed that the 6 amino acid sequences had highest similarity with 7S globulins from Leguminosae species, such as adzuki bean (*V. angularis*; ~86%), mung bean (*V. radiata*; ~86%), common bean (*Phaseolus vulgaris*; ~64%) and soybean (*Glycine* max; ~68%). Moreover, searches against the CDD showed that each protein contained two domains, both belonging to the cupin_1 family (SMART accession number: SM00835) of the cupin superfamily (Table S4). In the 6 cowpea proteins, the N- and C-terminal cupin_1 domains were 147 and 157 residues long, respectively. The cupin_1 family, which represents the conserved barrel domain of the cupin superfamily, contains 11S (legumins) and 7S (vicilins) seed storage globulins and germins [52]. Legumins and vicilins are two-domain proteins (bicupins), whereas germins are single-domain molecules (monocupins). This analysis showed that the cDNA sequences from cowpea encoded 6 proteins that have typical structural features of 7S seed storage globulins (Fig. 1).

To verify the relationship between the products encoded by the cDNA sequences and cowpea seed storage proteins, a fraction enriched in 7S globulins was obtained from mature seeds of both genotypes. When subjected to SDS-PAGE, the vicilin fractions from EPACE-10 and IT81D-1053 showed very similar profiles (Fig. S10). Each pattern was characterized by 11 protein bands, with apparent molecular masses ranging from 110 to 24 kDa, in which the bands with 60 and 54 kDa were the most abundant ones in each genotype. Almost all resolved bands (21 out of 22) were identified as 7-8S globulins by ESI-MS/MS (Tables S5 and S6). These results agree with previous works, which have demonstrated that under denaturing and reducing conditions, cowpea vicilins are a heterogeneous mixture of polypeptides of various sizes [53–55]. This pattern of polypeptides, characterized by distinct molecular masses, is typical of 7S globulins and probably arise by post-translational proteolytic processing of larger precursors, as demonstrated during the biosynthesis of vicilin, the 7S globulin of pea (*Pisum sativum*) seeds [56]. When the cowpea vicilin fractions were subjected to size exclusion chromatography, one main peak was obtained (PII; Fig. S11), which was further resolved into two peaks (PI and PII) by ion exchange chromatography (Fig. S12). Each major peak from the ion exchange chromatography showed a similar pattern of polypeptides, when analyzed by SDS-PAGE (Fig. S13), and both were enriched in the 60 and 54 kDa bands, which are characteristic of β-vignin, the major component of cowpea vicilin-like 7S globulins [57]. When these 2 major bands were subjected to Edman degradation, the same N-terminal amino acid sequence (26 residues) was obtained from both β-vignin bands of each genotype: IVHREHQESQEESEPRGQNNPFYFDS. This sequence matched exactly the first 26 amino acid residues deduced from the 6 partial cDNA fragments, which were obtained from developing seeds of cowpea. The average molecular mass calculated from these 6 sequences was, approximately, 49.7 kDa, which is closer to the faster migrating β-vignin subunit. The differences between the values calculated from the sequences and those determined by SDS-PAGE are probably due to glycosylation. Indeed, some authors have demonstrated that the 2 main β-vignin polypeptides are both glycosylated, the 60 kDa subunit having a greater amount of carbohydrate than the 54 kDa subunit [57,58]. To further strength the relationship between the sequences deduced from the cDNA fragments and the proteins purified from cowpea seeds, several tryptic peptides were identified by MALDI-TOF MS analysis from the 2 major peaks resolved by ion exchange chromatography (Figs. S14–S18). The sequences of these peptides matched specific segments of the primary structures deduced from the cDNA fragments obtained from IT81D-1053 (Table S7) and EPACE-10 (Table S8). The experimentally determined peptides covered approximately 23.4 and 17.6% of the amino acid sequences of the proteins from EPACE1–10 and IT81D-1053,

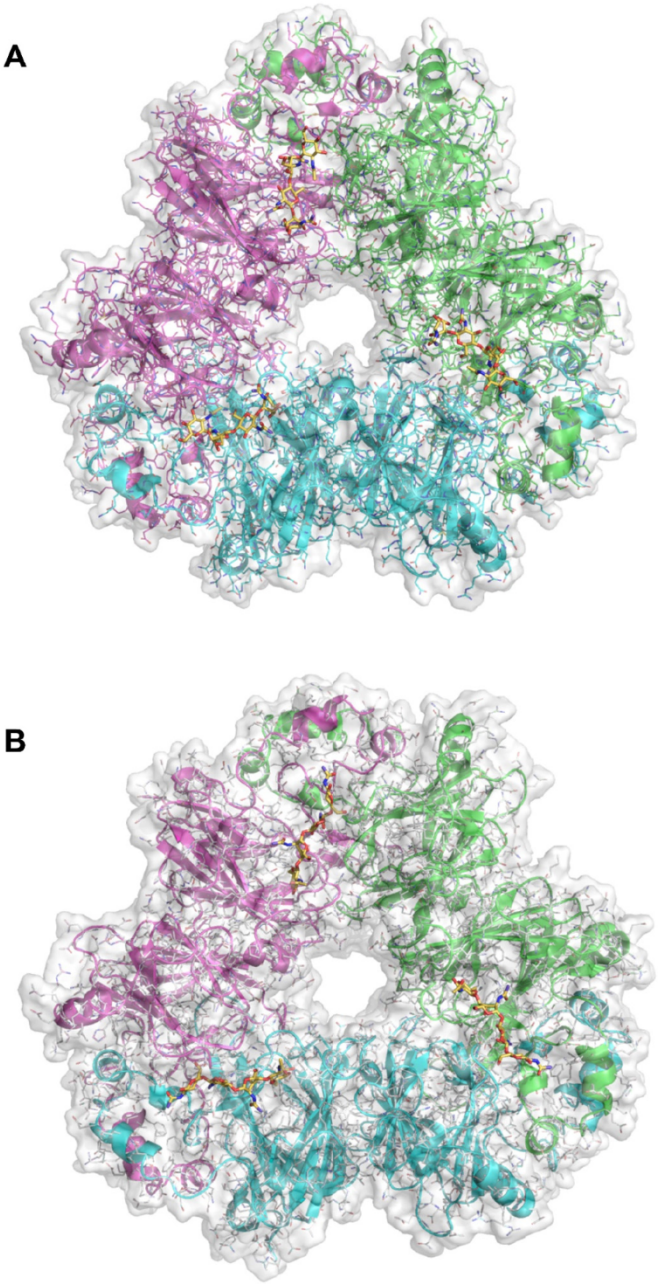

Fig. 3. Ribbon diagrams of the β-vignin homotrimers. Homotrimers of the models S2 (A) and R2 (B) are shown. Subunits are colored pink, green and cyan. Chito-oligosaccharide molecules [$(GlcNAc)_4$] docked in the chitin-binding sites of each oligomer are also shown as stick models (carbon, nitrogen and oxygen atoms are colored yellow, blue and red, respectively). (For interpretation of the references to color in this figure legend, the reader is referred to the web version of this article.)

respectively. Therefore, the cDNA fragments cloned from EPACE-10 and IT81D-1053 encode β-vignin, which is the main fraction of the 7S globulins stored in cowpea seeds.

3.2. Molecular models of β-vignin and their interaction with chitin oligomers

To investigate how cowpea vicilins bind chitin, three-dimensional molecular models were generated, refined, validated and subjected to computational simulations using chito-oligosaccharides as potential ligands. Vicilin models were built from 4 amino acid sequences (S2 and S3 from EPACE-10 and R2 and R3 from IT81D-1053), using the three-dimensional structure of the 7S globulin-1 (PDB ID: 2EA7) from adzuki bean (*V. angularis*) as template (Figs. S19–S22; average sequence identity percentages between the primary structures of β-vignin and adzuki bean 7S globulin-1 were, approximately, 83.1%). When the modeled structures (designated as models S2, S3, R2 and R3) were aligned, an RMSD of 1.479 Å was obtained (Fig. S23), indicating that the models had very similar folds. Furthermore, superposition of the model and template structures gave the following TM-score values: 0.7224 (model S2 *vs* 2EA7), 0.5013 (model S3 *vs* 2EA7), 0.7245 (model R2 *vs* 2EA7) and 0.7199 (model R3 *vs* 2EA7). This analysis showed that the overall fold of the modeled structures was correct (Fig. 2), as indicated by the TM-score values >0.5 [59]. In the three-dimensional structures of the β-vignin models, the N- and C-terminal halves of the polypeptide chain assumed the characteristic cupin fold, the domains being symmetrically related by a pseudo-twofold axis, and each one containing a core β-barrel and an extended loop region with 2 helices (Fig. 2), as typically found in 7S globulins [40]. After refinement, the percentage of Ramachandran outliers was either 0 or <1%. Clashscore, which is the number of clashes ≥0.4 Å per 1000 atoms, ranged from 6.65 (88th percentile) to 13.52 (56th percentile), whereas MolProbity score varied from 1.38 (97th percentile) to 1.71 (89th percentile) (Tables S9-S12). MolProbity score is a log-weighted combination of the clashscore, percentage of Ramachandran outliers and percentage of bad side-chain rotamers, providing one value that reflects the approximate crystallographic resolution at which that combination of numbers would be expected [42]. Therefore, the molecular models of cowpea vicilins were judged as of good quality, according to MolProbity validation criteria.

In native 7S globulins, monomers assemble into trimers, in which the subunits are held by non-covalent forces. These trimers have a triangle-like shape, arising through head-to-tail association of individual monomers [40]. Symmetry operations were used to generate β-vignin homotrimers, and these oligomers were subjected to computational simulations. Initial molecular docking calculations suggested that each trimer of β-vignin had 3 sites that could bind chito-oligosaccharides. These binding sites were located at the vertices of the triangle-shaped oligomer, and each one was constituted by some residues from one subunit and other residues from its neighbor chain (Fig. 3). To verify the stability of a tetra-*N*-acetyl-chitotetraose molecule docked in a single binding site of cowpea β-vignins, molecular dynamics simulations were performed. RMSD plots showed that, after an initial accommodation that took place in the first nanoseconds, the interaction of the bound oligosaccharide was very stable along most simulations, especially in the complexes between $(GlcNAc)_4$ and the models S3 and R2 (Fig. S24). In the stable complexes obtained after MD

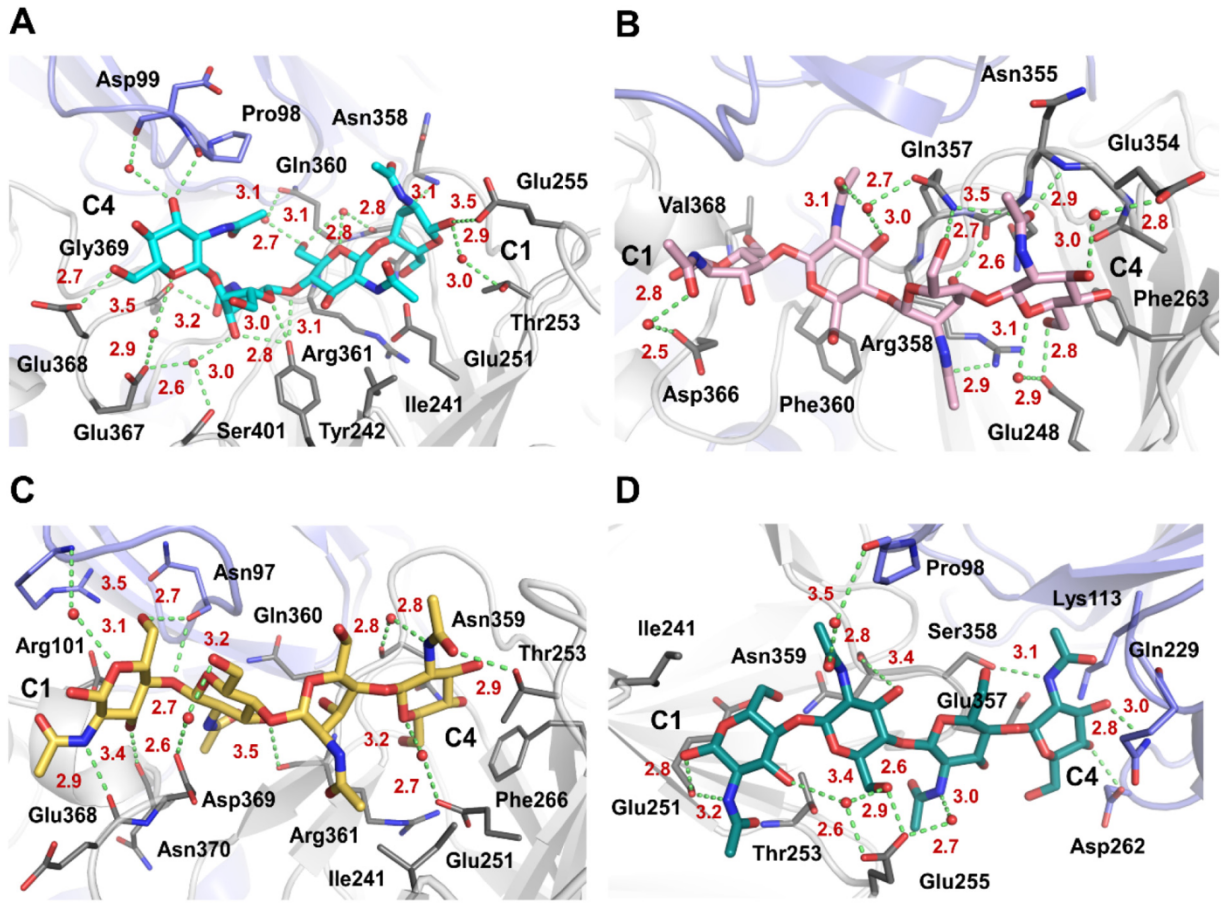

Fig. 4. Close-up view of a $(GlcNAc)_4$ molecule docked in the chitin-binding site of β-vignin. The panels show a ligand molecule docked in the ChBS of models S2 (A), S3 (B), R2 (C) and R3 (D). Water molecules are represented as red spheres, hydrogen bonds are shown as green dotted lines (the distance cut-off is 3.5 Å) and the side chains of interacting residues are depicted as sticks. C1 and C4 indicate the carbon atoms of the monosaccharide units from the reducing and non-reducing ends, respectively. Nitrogen and oxygen atoms are colored blue and red, respectively. (For interpretation of the references to color in this figure legend, the reader is referred to the web version of this article.)

simulations, the interaction between amino acid residues and ligand atoms was mediated mainly by hydrogen bonds and hydrophobic contacts (Fig. 4). In each complex, a network of hydrogen bonds was observed, involving hydroxyl groups from each GlcNAc unit of the bound oligosaccharide and several O and N atoms from the side chains of some residues of the modeled protein structure. Many of these polar interactions between the chito-oligosaccharide and β-vignin were predicted to be mediated by water molecules (Fig. 5). Carbohydrate-binding proteins, including a large diversity of enzymes as well as non-enzymatic proteins, such as lectins, have wide differences in their three-dimensional structures and carbohydrate-binding topologies. However, a common feature of the interactions between proteins and their carbohydrate ligands is the prevalence of hydrogen bond interactions, usually involving water molecules [60]. Most of the β-vignin amino acid residues, involved in the interactions with the bound oligosaccharide in each chitin binding-site (ChBS), were mapped to 4 main

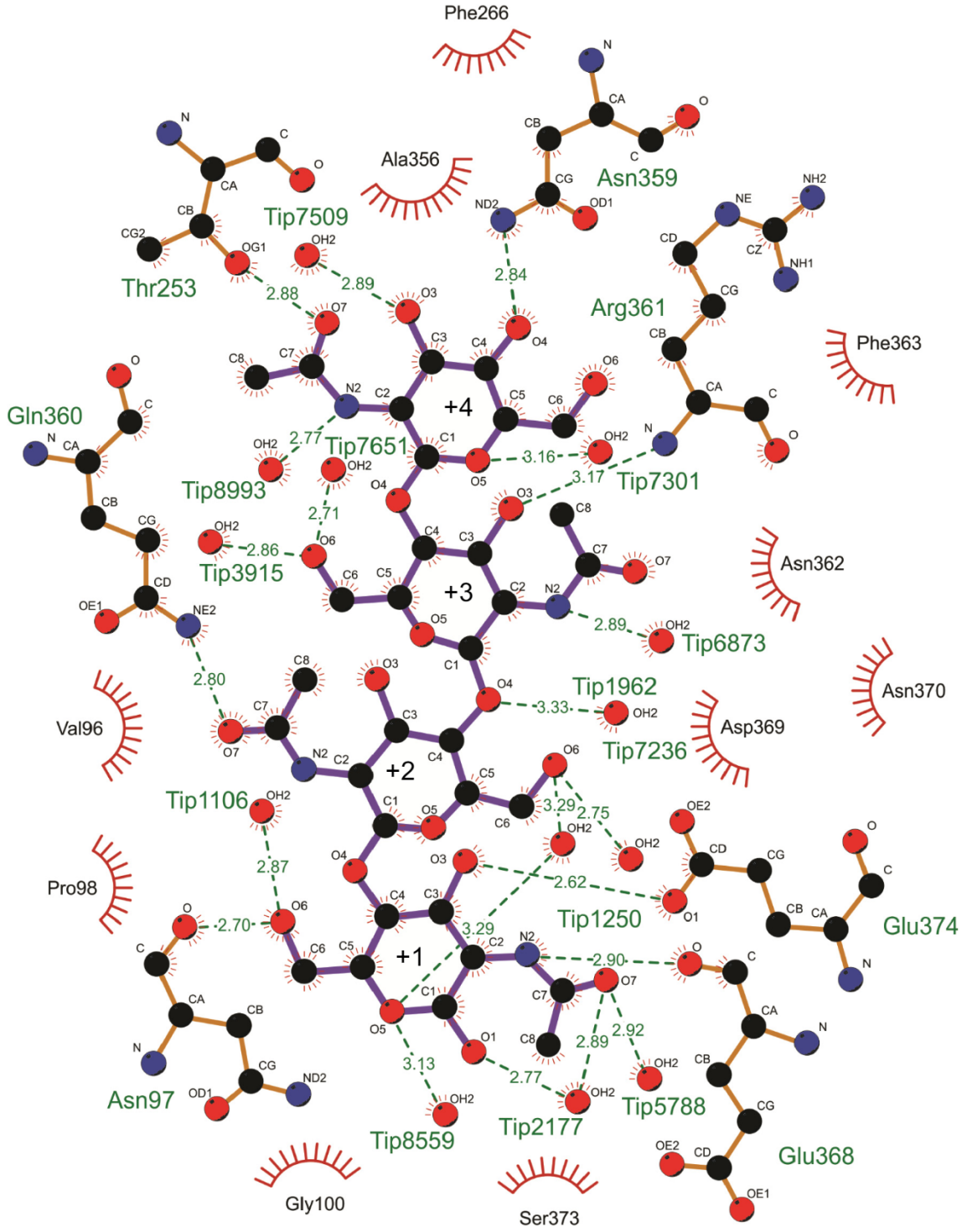

Fig. 5. Two-dimensional diagram of the interaction model between a $(GlcNAc)_4$ molecule docked in the chitin-binding site of β-vignin. Residues from model R2 involved in hydrogen bonds (green dashed lines) or hydrophobic contacts (brick-red spoked arcs) are shown. Water molecules (labeled OH_2) are represented as red spheres. Monosaccharide units are numbered from +1 (reducing end) to +4 (non-reducing end). Similar diagrams depicting the interaction models obtained for the other complexes are shown in Figs. S25–S27. The diagrams were generated using the program LigPlot+ [65]. (For interpretation of the references to color in this figure legend, the reader is referred to the web version of this article.)

segments in the protein's primary structure (Fig. 1). One of these segments was mapped in the N-terminal domain, whereas the other 3 regions were constituted by residues found in the C-terminal domain. Some of the residues from these 4 regions that were involved in the interaction between β-vignin and chito-oligosaccharides are conserved in other 7S globulins. Using a quantum mechanics-based method, the binding free energies of chito-oligosaccharide molecules to β-vignin oligomers were calculated, ranging from −690.6 kcal/mol (GlcNAc oligomers bound to β-vignin R2 trimer) to −531.3 kcal/mol (chitin fragments bound to β-vignin R3 oligomer) (Table S13). These results agree with previous works, which have demonstrated that cowpea vicilins purified from seeds of genotypes that are susceptible or resistant to *C. maculatus* have the ability to bind *in vitro* to chitin [17] and *in vivo* to chitinous structures of the larvae's midgut [18,19]. Furthermore, the conservation in other 7S globulins of many of the residues that constitute the β-vignin's ChBS, as predicted in this work, also support earlier reports that have shown that vicilins from other leguminous species can also bind to chitin [61]. Quantum mechanical (QM) interaction energy, calculated between model R2 and $(GlcNAc)_4$ molecules, was lower (−690.6 kcal/mol) than that predicted between model S3 complexed with the same oligosaccharide (−542.1 kcal/mol) (Table S13), the difference between them being approximately −149 kcal/mol. Although QM interaction energies are much larger than the actual experimental values, a good correlation between them has been found, and this approach has a better performance in rank-ordering binding affinities when compared to other methods [62]. This suggested that R3 trimers are expected to bind chitin oligomers with higher affinity in comparison to S3 oligomers. These data raised the possibility that variant vicilins with differential binding affinities to chitin oligomers may be expressed in cowpea seeds which show contrasting responses when infested by *C. maculatus* larvae, and these differences in binding affinity could explain, at least in part, the deleterious effects of cowpea vicilins from resistant genotypes on bruchid's larvae. However, these assumptions need further investigations.

7S globulins are major storage proteins of leguminous seeds, providing amino acid skeletons for the growing seedling after germination. Besides this fundamental role, evidences have suggested that these proteins may be involved in other biological functions, such as defense mechanisms. Cowpea vicilins, for example, bind chitin, a polysaccharide of β-1,4 linked GlcNAc units that is found in the exoskeleton of insects, crustaceans and other invertebrates. Chitin is also an important component of the peritrophic membrane, a tube-like structure that covers the midgut epithelium of insects. Bruchid beetles, such as *C. maculatus* and *Z. subfasciatus*, apparently do not have a peritrophic membrane, but contain a peritrophic gel along the whole midgut [63], and the presence of chitinous structures in the peritrophic gel of *C. maculatus* larvae has been demonstrated [19]. The ability of cowpea vicilins to interact with chitin has been implicated in the resistance of some genotypes to *C. maculatus*. However, the binding mode of these storage proteins to this polymer has remained unknown. The analysis performed in the present study suggested a molecular mechanism that explains how cowpea vicilins bind chitin and hence affect the larval development of bruchid beetles. Due to conservation of the primary, tertiary and quaternary structures of 7S globulins, the proposed mechanism is likely to apply to chitin-binding vicilins from other species.

4. Conclusions

Partial cDNA sequences encoding β-vignin, the main component of the 7S globulins of cowpea, were obtained. Computational simulations were then used to predict the probable chitin-binding sites in the modeled structures. Interaction models suggested that chito-oligosaccharides bound to β-vignin are stabilized mainly by hydrogen bonds, a typical structural feature of many carbohydrate-binding proteins.

Acknowledgements

This work was supported by research grants from Conselho Nacional de Desenvolvimento Científico e Tecnológico (CNPq), Coordenação de Aperfeiçoamento de Pessoal de Nível Superior (CAPES) and Fundação Cearense de Apoio ao Desenvolvimento Científico e Tecnológico (FUNCAP). AJR was recipient of Doctoral Fellowships from CAPES and CNPq. TBG is a senior researcher (PQ-2) of CNPq.

Appendix A. Supplementary data

Supplementary data to this article can be found online at https://doi.org/10.1016/j.ijbiomac.2018.05.197.

References

[1] J.D. Ehlers, A.E. Hall, Cowpea (*Vigna unguiculata* L. Walp.), Field Crop Res. 53 (1997) 187–204, https://doi.org/10.1016/S0378-4290(97)00031-2.
[2] B.B. Singh, H.A. Ajeigbe, S.A. Tarawali, S. Fernandez-Rivera, M. Abubakar, Improving the production and utilization of cowpea as food and fodder, Field Crop Res. 84 (2003) 169–177, https://doi.org/10.1016/S0378-4290(03)00148-5.
[3] R.W. Howe, J.E. Currie, Some laboratory observations on the rates of development, mortality and oviposition of several species of Bruchidae breeding in stored pulses, Bull. Entomol. Res. 55 (1964) 437–477, https://doi.org/10.1017/S0007485300049580.
[4] L.L. Murdock, D. Seck, G. Ntoukam, L. Kitch, R.E. Shade, Preservation of cowpea grain in sub-Saharan Africa - bean/cowpea CRSP contributions, Field Crop Res. 82 (2003) 169–178, https://doi.org/10.1016/S0378-4290(03)00036-4.
[5] P.C. Ojimelukwe, F.C. Ogwumike, Effects of infestation by bruchid beetles (*Callosobruchus macultus*) on the nutritional quality and sensory properties of cowpeas (*Vigna unguiculata*), J. Food Biochem. 23 (1999) 637–645.
[6] R.A. Melo, V.A. Forti, S.M. Cicero, A.D.L.C. Novembre, P.C.T. Melo, Use of X-ray to evaluate damage caused by weevils in cowpea seeds, Hortic. Bras. 28 (2010) 472–476, https://doi.org/10.1590/S0102-05362010000400016.
[7] B.B. Singh, S.R. Singh, O. Adjadi, Bruchid resistance in cowpea, Crop Sci. 25 (1985) 736–739.
[8] B.B. Singh, S.R. Singh, Breeding for bruchid resistance in cowpea, in: K. Fujii, A.M.R. Gatehouse, C.D. Johnson, R. Mitchel, T. Yoshida (Eds.), Bruchids and Legumes: Economics, Ecology and Coevolution, Kluwer Academic Publishers, Dordrecht 1990, pp. 219–228.
[9] A.M.R. Gatehouse, J.A. Gatehouse, P. Dobie, A.M. Kilminster, D. Boulter, Biochemical basis of insect resistance in *Vigna unguiculata*, J. Sci. Food Agric. 30 (1979) 948–958, https://doi.org/10.1002/jsfa.2740301003.
[10] A.M.R. Gatehouse, D. Boulter, Assessment of the antimetabolic effects of trypsin inhibitors from cowpea (*Vigna unguiculata*) and other legumes on development of the bruchid beetle *Callosobruchus maculatus*, J. Sci. Food Agric. 34 (1983) 345–350, https://doi.org/10.1002/jsfa.2740340405.
[11] T.A. Baker, N. Suzanne, R.E. Shade, B.B. Singh, Physical and chemical attributes of cowpea lines resistant and susceptible to *Callosobruchus maculatus* (F.) (Coleoptera: Bruchidae), J. Stored Prod. Res. 25 (1989) 1–8, https://doi.org/10.1016/0022-474X(89)90002-7.
[12] J. Xavier-Filho, F.A.P. Campos, M.B. Ary, C.P. Silva, M.M.M. Carvalho, M.L.R. Macedo, F.J.A. Lemos, G. Grant, Poor correlation between the levels of proteinase inhibitors found in seeds of different cultivars of cowpea (*Vigna unguiculata*) and the resistance/susceptibility to predation by *Callosobruchus maculatus*, J. Agric. Food Chem. 37 (1989) 1139–1143, https://doi.org/10.1021/jf00088a071.
[13] K.V. Fernandes, P.A. Sabelli, D.H. Barratt, M. Richardson, J. Xavier-Filho, P.R. Shewry, The resistance of cowpea seeds to bruchid beetles is not related to levels of cysteine proteinase inhibitors, Plant Mol. Biol. 23 (1993) 215–219.
[14] C.M. Reis, M.M. Calvet, M.P. Sales, K.V.S. Fernandes, V.M. Gomes, J. Xavier, α-Amylase inhibitors of legume seeds and their involvement in the resistance to Bruchid beetles, Arq. Biol. E Tecnol. 40 (1997) 413–418.
[15] M.P. Sales, M.L.R. Macedo, J. Xavier-Filho, Digestibility of cowpea (*Vigna unguiculata*) vicilins by pepsin, papain and bruchid (insect) midgut proteinases, Comp. Biochem. Physiol. B Biochem. Mol. Biol. 103 (1992) 945–950, https://doi.org/10.1016/0305-0491(92)90220-L.
[16] M.L.R. Macedo, S.L.B. Da Andrade, R.A. Moraes, J. Xavier-Filho, Vicilin variants and the resistance of cowpea (*Vigna unguiculata*) seeds to the cowpea weevil (*Callosobruchus maculatus*), Comp. Biochem. Physiol. C: Toxicol. Pharmacol. 105 (1993) 89–94, https://doi.org/10.1016/0742-8413(93)90063-Q.
[17] M.P. Sales, V.M. Gomes, K.V.S. Fernandes, J. Xavier, Chitin-binding proteins from cowpea (*Vigna unguiculata*) seeds, Braz. J. Med. Biol. Res. 29 (1996) 319–326.
[18] F. Firmino, K.V.S. Fernandes, M.P. Sales, V.M. Gomes, M.R.A. Miranda, S.J.S. Domingues, J. Xavier, Cowpea (*Vigna unguiculata*) vicilins associate with putative chitinous structures in the midgut and feces of the bruchid beetles *Callosobruchus maculatus* and *Zabrotes subfasciatus*, Braz. J. Med. Biol. Res. 29 (1996) 749–756.
[19] M.P. Sales, P.P. Pimenta, N.S. Paes, M.F. Grossi-De-Sa, J. Xavier, Vicilins (7S storage globulins) of cowpea (*Vigna unguiculata*) seeds bind to chitinous structures of the midgut of *Callosobruchus maculatus* (Coleoptera: Bruchidae) larvae, Braz. J. Med. Biol. Res. 34 (2001) 27–34, https://doi.org/10.1590/S0100-879X2001000100003.
[20] A.F. Uchôa, R.A. Damatta, C.A. Retamal, J.M. Albuquerque-Cunha, S.M. Souza, R.I. Samuels, C.P. Silva, J. Xavier, Presence of the storage seed protein vicilin in internal

organs of larval *Callosobruchus maculatus* (Coleoptera: Bruchidae), J. Insect Physiol. 52 (2006) 169–178, https://doi.org/10.1016/j.jinsphys.2005.10.002.
[21] S.M. Souza, A.F. Uchôa, J.R. Silva, R.I. Samuels, A.E.A. Oliveira, E.M. Oliveira, R.T. Linhares, D. Alexandre, C.P. Silva, The fate of vicilins, 7S storage globulins, in larvae and adult *Callosobruchus maculatus* (Coleoptera: Chrysomelidae: Bruchinae), J. Insect Physiol. 56 (2010) 1130–1138, https://doi.org/10.1016/j.jinsphys.2010.03.009.
[22] G.B. Oliveira, D. Kunz, T.V. Peres, R.B. Leal, A.F. Uchôa, R.I. Samuels, M.L.R. Macedo, C.R. Carlini, A.F. Ribeiro, T.B. Grangeiro, W.R. Terra, J. Xavier-Filho, C.P. Silva, Variant vicilins from a resistant *Vigna unguiculata* lineage (IT81D-1053) accumulate inside *Callosobruchus maculatus* larval midgut epithelium, Comp. Biochem. Physiol. B Biochem. Mol. Biol. 168 (2014) 45–52, https://doi.org/10.1016/j.cbpb.2013.11.001.
[23] D. Kunz, G.B. Oliveira, A.F. Uchôa, R.I. Samuels, M.L.R. Macedo, C.P. Silva, Receptor mediated endocytosis of vicilin in *Callosobruchus maculatus* (Coleoptera: Chrysomelidae) larval midgut epithelial cells, Comp. Biochem. Physiol. B Biochem. Mol. Biol. 210 (2017) 39–47, https://doi.org/10.1016/j.cbpb.2017.06.003.
[24] M.P. Sales, L.B.S. Andrade, M.B. Ary, M.R.A. Miranda, F.M. Teixeira, A.S. Oliveira, K.V.S. Fernandes, J. Xavier, Performance of bean bruchids *Callosobruchus maculatus* and *Zabrotes subfasciatus* (Coleoptera: Bruchidae) reared on resistant (IT81D-1045) and susceptible (Epace 10) *Vigna unguiculata* seeds: relationship with trypsin inhibitor and vicilin excretion, Comp. Biochem. Physiol. A Mol. Integr. Physiol. 142 (2005) 422–426, https://doi.org/10.1016/j.cbpa.2005.09.005.
[25] J. Meik, P. Dobie, The ability of *Zabrotes subfasciatus* to attack cowpeas, Entomol. Exp. Appl. 42 (1986) 151–158, https://doi.org/10.1111/j.1570-7458.1986.tb01016.x.
[26] J.M. Dunwell, A. Purvis, S. Khuri, Cupins: the most functionally diverse protein superfamily? Phytochemistry 65 (2004) 7–17.
[27] S. Chang, J. Puryear, J. Cairney, A simple and efficient method for isolating RNA from pine trees, Plant Mol. Biol. Report. 11 (1993) 113–116, https://doi.org/10.1007/BF02670468.
[28] P.A.C. Maranhão, C.S. Teixeira, B.L. Sousa, I.L. Barroso-Neto, J.E. Monteiro-Júnior, A.V. Fernandes, M.V. Ramos, I.M. Vasconcelos, J.F.C. Gonçalves, B.A.M. Rocha, V.N. Freire, T.B. Grangeiro, cDNA cloning, molecular modeling and docking calculations of L-type lectins from *Swartzia simplex* var. grandiflora (Leguminosae, Papilionoideae), a member of the tribe Swartzieae, Phytochemistry 139 (2017) 60–71, https://doi.org/10.1016/j.phytochem.2017.04.007.
[29] T.A. Hall, BioEdit: a user-friendly biological sequence alignment editor and analysis program for Windows 95/98/NT, Nucleic Acids Symp. Ser. 41 (1999) 95–98.
[30] S.F. Altschul, W. Gish, W. Miller, E.W. Myers, D.J. Lipman, Basic local alignment search tool, J. Mol. Biol. 215 (1990) 403–410.
[31] R.H. Sammour, J.A. Gatehouse, J. Gilroy, D. Boulter, The homology of the major storage protein of jack bean (*Canavalia ensiformis*) to pea vicilin and its separation from α-mannosidase, Planta 161 (1984) 61–70, https://doi.org/10.1007/BF00951461.
[32] U.K. Laemmli, Cleavage of structural proteins during the assembly of the head of bacteriophage T4, Nature 227 (1970) 680–685.
[33] M.D. Lobo, F.D. Silva, P.G. Landim, P.R. da Cruz, T.L. de Brito, S.C. de Medeiros, J.T. Oliveira, I.M. Vasconcelos, H.D. Pereira, T.B. Grangeiro, Expression and efficient secretion of a functional chitinase from *Chromobacterium violaceum* in *Escherichia coli*, BMC Biotechnol. 13 (2013) 46, https://doi.org/10.1186/1472-6750-13-46.
[34] P.G.C. Landim, T.O. Correia, F.D.A. Silva, D.R. Nepomuceno, H.P.S. Costa, H.M. Pereira, M.D.P. Lobo, F.B.M.B. Moreno, J. Brandão-Neto, S.C. Medeiros, I.M. Vasconcelos, J.T.A. Oliveira, B.L. Sousa, I.L. Barroso-Neto, V.N. Freire, C.P.S. Carvalho, A.C.O. Monteiro-Moreira, T.B. Grangeiro, Production in Pichia pastoris, antifungal activity and crystal structure of a class I chitinase from cowpea (*Vigna unguiculata*): insights into sugar binding mode and hydrolytic action, Biochimie 135 (2017) 89–103, https://doi.org/10.1016/j.biochi.2017.01.014.
[35] A. Shevchenko, H. Tomas, J. Havlis, J.V. Olsen, M. Mann, In-gel digestion for mass spectrometric characterization of proteins and proteomes, Nat. Protoc. 1 (2006) 2856–2860, https://doi.org/10.1038/nprot.2006.468.
[36] J.E.C. Freire, I.M. Vasconcelos, F.B.M.B. Moreno, A.B. Batista, M.D.P. Lobo, M.L. Pereira, J.P.M.S. Lima, R.V.M. Almeida, A.J.S. Sousa, A.C.O. Monteiro-Moreira, J.T.A. Oliveira, T.B. Grangeiro, Mo-CBP3, an antifungal chitin-binding protein from *Moringa oleifera* seeds, is a member of the 2S albumin family, PLoS One 10 (2015), e0119871. https://doi.org/10.1371/journal.pone.0119871.
[37] E. Gasteiger, C. Hoogland, A. Gattiker, S. Duvaud, M. Wilkins, R. Appel, A. Bairoch, Protein identification and analysis tools on the ExPASy server, in: J.M. Walker (Ed.), The Proteomics Protocols Handbook, Humana Press, Totowa 2005, pp. 571–607.
[38] A. Sali, L. Potterton, F. Yuan, H. van Vlijmen, M. Karplus, Evaluation of comparative protein modeling by MODELLER, Proteins 23 (1995) 318–326, https://doi.org/10.1002/prot.340230306.
[39] V. Alva, S.-Z. Nam, J. Söding, A.N. Lupas, The MPI bioinformatics toolkit as an integrative platform for advanced protein sequence and structure analysis, Nucleic Acids Res. 44 (2016) W410–W415, https://doi.org/10.1093/nar/gkw348.
[40] T. Fukuda, N. Maruyama, M.R.M. Salleh, B. Mikami, S. Utsumi, Characterization and crystallography of recombinant 7S globulins of adzuki bean and structure-function relationships with 7S globulins of various crops, J. Agric. Food Chem. 56 (2008) 4145–4153, https://doi.org/10.1021/jf072667b.
[41] L. Heo, H. Park, C. Seok, GalaxyRefine: protein structure refinement driven by side-chain repacking, Nucleic Acids Res. 41 (2013) W384–W388, https://doi.org/10.1093/nar/gkt458.
[42] V.B. Chen, W.B. Arendall, J.J. Headd, D.A. Keedy, R.M. Immormino, G.J. Kapral, L.W. Murray, J.S. Richardson, D.C. Richardson, MolProbity: all-atom structure validation for macromolecular crystallography, Acta Crystallogr. D Biol. Crystallogr. 66 (2010) 12–21, https://doi.org/10.1107/S0907444909042073.
[43] O. Trott, A.J. Olson, AutoDock Vina: improving the speed and accuracy of docking with a new scoring function, efficient optimization, and multithreading, J. Comput. Chem. 31 (2010) 455–461, https://doi.org/10.1002/jcc.21334.
[44] A. Bohne, E. Lang, C.W. von der Lieth, SWEET - WWW-based rapid 3D construction of oligo- and polysaccharides, Bioinformatics 15 (1999) 767–768.
[45] G.M. Morris, R. Huey, W. Lindstrom, M.F. Sanner, R.K. Belew, D.S. Goodsell, A.J. Olson, AutoDock4 and AutoDockTools4: automated docking with selective receptor flexibility, J. Comput. Chem. 30 (2009) 2785–2791, https://doi.org/10.1002/jcc.21256.
[46] J.C. Phillips, R. Braun, W. Wang, J. Gumbart, E. Tajkhorshid, E. Villa, C. Chipot, R.D. Skeel, L. Kalé, K. Schulten, Scalable molecular dynamics with NAMD, J. Comput. Chem. 26 (2005) 1781–1802, https://doi.org/10.1002/jcc.20289.
[47] R.B. Best, X. Zhu, J. Shim, P.E.M. Lopes, J. Mittal, M. Feig, A.D. Mackerell, Optimization of the additive CHARMM all-atom protein force field targeting improved sampling of the backbone φ, ψ and side-chain χ(1) and χ(2) dihedral angles, J. Chem. Theory Comput. 8 (2012) 3257–3273, https://doi.org/10.1021/ct300400x.
[48] O. Guvench, S.S. Mallajosyula, E.P. Raman, E. Hatcher, K. Vanommeslaeghe, T.J. Foster, F.W. Jamison, A.D. Mackerell, CHARMM additive all-atom force field for carbohydrate derivatives and its utility in polysaccharide and carbohydrate-protein modeling, J. Chem. Theory Comput. 7 (2011) 3162–3180, https://doi.org/10.1021/ct200328p.
[49] W. Humphrey, A. Dalke, K. Schulten, VMD: visual molecular dynamics, J. Mol. Graph. 14 (1996) 33–38 (27–28).
[50] B. Delley, From molecules to solids with the DMol3 approach, J. Chem. Phys. 113 (2000) 7756–7764, https://doi.org/10.1063/1.1316015.
[51] C. Li, Y.-M. Zhang, Molecular evolution of glycinin and β-conglycinin gene families in soybean (*Glycine max* L. Merr.), Heredity 106 (2011) 633–641, https://doi.org/10.1038/hdy.2010.97.
[52] J.M. Dunwell, Cupins: a new superfamily of functionally diverse proteins that include germins and plant storage proteins, Biotechnol. Genet. Eng. Rev. 15 (1998) 1–32.
[53] A.L. Cerdeira, A.W. Cole, D.S. Luthe, Cowpea (*Vigna unguiculata*) seed protein response to glyphosate, Weed Sci. 33 (1985) 1–6, https://doi.org/10.1017/S0043174500083843.
[54] M.R.I. Khan, J.A. Gatehouse, D. Boulter, The seed proteins of cowpea (*Vigna unguiculata* L. Walp.), J. Exp. Bot. 31 (1980) 1599–1611.
[55] D.R. Murray, K.F. Mackenzie, F. Vairinhos, M.B. Peoples, C.A. Atkins, J.S. Pate, Electrophoretic studies of the seed proteins of cowpea, *Vigna unguiculata* (L.) Walp, Z. Pflanzenphysiol. 109 (1983) 363–370, https://doi.org/10.1016/S0044-328X(83)80118-4.
[56] M.J. Chrispeels, T.J. Higgins, D. Spencer, Assembly of storage protein oligomers in the endoplasmic reticulum and processing of the polypeptides in the protein bodies of developing pea cotyledons, J. Cell Biol. 93 (1982) 306–313.
[57] R.L. Freitas, A.R. Teixeira, R.B. Ferreira, Characterization of the proteins from *Vigna unguiculata* seeds, J. Agric. Food Chem. 52 (2004) 1682–1687, https://doi.org/10.1021/jf0300588.
[58] E. de Souza Ferreira, J. Capraro, F. Sessa, C. Magni, A. Demonte, A. Consonni, V. Augusto Neves, E. Maffud Cilli, M. Duranti, A. Scarafoni, New molecular features of cowpea bean (*Vigna unguiculata*, l. Walp) β-vignin, Biosci. Biotechnol. Biochem. 82 (2018) 285–291, https://doi.org/10.1080/09168451.2017.1419855.
[59] Y. Zhang, J. Skolnick, Scoring function for automated assessment of protein structure template quality, Proteins 57 (2004) 702–710, https://doi.org/10.1002/prot.20264.
[60] F.A. Quiocho, Carbohydrate-binding proteins: tertiary structures and protein-sugar interactions, Annu. Rev. Biochem. 55 (1986) 287–315, https://doi.org/10.1146/annurev.bi.55.070186.001443.
[61] L.L.P. Macedo, T.M.L. Amorim, A.F. Uchôa, A.S. Oliveira, J.K.C. Ribeiro, F.P. de Macedo, E.A. Santos, M.P. de Sales, Larvicidal effects of a chitin-binding vicilin from *Erythrina velutina* seeds on the mediterranean fruit fly Ceratitis capitata, J. Agric. Food Chem. 56 (2008) 802–808, https://doi.org/10.1021/jf072746n.
[62] M. Chen, H. Hiang, X. Lin, Y. Chen, M. Wang, J. Liu, DFT study of binding energies between acetohydroxyacid synthase and its sulfonylurea inhibitors: an application of quantum pseudoreceptor model, Commun. Comput. Chem. 1 (2013) 72–87, https://doi.org/10.4208/cicc.2013.v1.n1.8.
[63] W.R. Terra, The origin and functions of the insect peritrophic membrane and peritrophic gel, Arch. Insect Biochem. Physiol. 47 (2001) 47–61, https://doi.org/10.1002/arch.1036.
[64] C.S. Bond, A.W. Schüttelkopf, ALINE: a WYSIWYG protein-sequence alignment editor for publication-quality alignments, Acta Crystallogr. D Biol. Crystallogr. 65 (2009) 510–512, https://doi.org/10.1107/S0907444909007835.
[65] R.A. Laskowski, M.B. Swindells, LigPlot+: multiple ligand-protein interaction diagrams for drug discovery, J. Chem. Inf. Model. 51 (2011) 2778–2786, https://doi.org/10.1021/ci200227u.